Supplementary information of
The growing seasons of global forest ecosystems from 1850 to 2100 estimated with a probabilistic temperature-based model

Pierluigi R. Guaita, Giacomo Gerosa, Riccardo Marzuoli

[1]Department of Mathematics and Physics, Catholic University of the Sacred Heart, Brescia, Italy
[2]Department of Applied Computational Mathematics and Statistics, University of Notre Dame, Notre Dame, IN, USA

Correspondence to: pierluigirenan.guaita@unicatt.it, giacomo.gerosa@unicatt.it

Table S1. Criteria to define areas according to the KG classification, using only temperature. T_{hot} and T_{cold} are the climatologically warmest and the coldest months, respectively. T_{mon10} indicates the number of months with a temperature above 10°C.

Main group	Subgroup	Criteria
C (temperate)		$0°C<T_{cold}<18°C \wedge T_{hot} > 10°C$
	C*a (subtropical/hot summer Mediterranean)	$T_{hot} \geq 22°C$
	C*b (warm-summer Mediterranean/Oceanic/dry-winter subtropical)	$not(C*a) \wedge T_{hot10} \geq 4$ mo
	C*c (cold-summer Mediterranean/subpolar oceanic/dry-winter cold subtropical highland)	$not(C*a \vee C*b) \wedge 1$ mo $\leq T_{mon10} \leq 4$ mo
D (continental)		$T_{hot} > 10°C \wedge T_{cold} \leq 0°C$
	D*a (hot summer)	$T_{hot} \geq 22°C$
	D*b (warm summer)	$not(D*a) \wedge T_{mon10} \geq 4$ mo
	D*c (subarctic)	$not(D*a \vee D*b \vee D*d)$
	D*d (subarctic with sever winter)	$not(D*a \vee D*b) \wedge T_{cold}<-38°C$

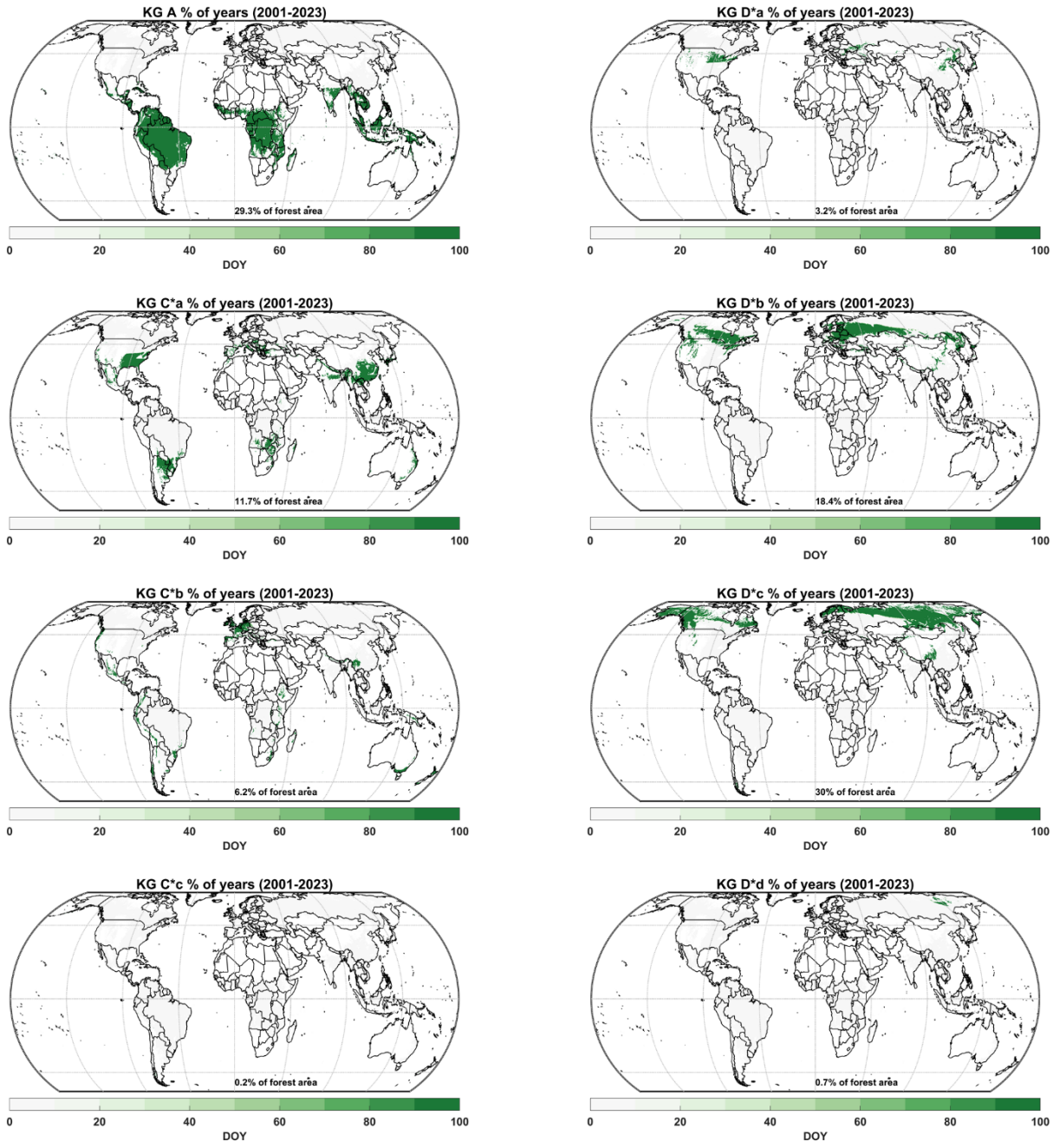

Figure S1. Percentage of the years 2001-2023 falling within each KG classification from the ERA5 temperatures. Note that climatological shifts lead to transitions between KG classes.

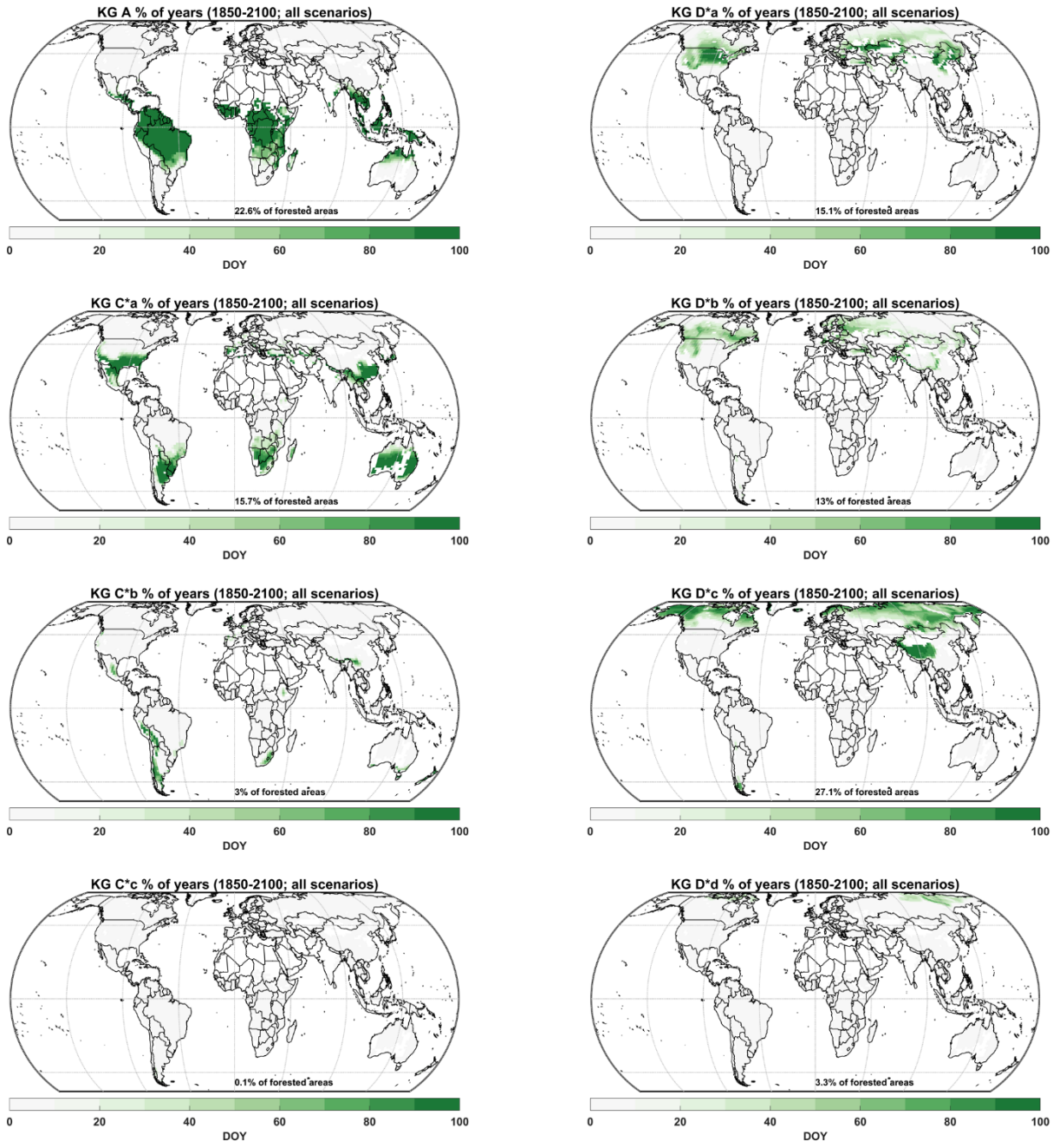

Figure S2. Percentage of the years 1850-2100 (jointly historical, SSP1-2.6, SSP3-7.0, and SSP5-8.5 experiments) falling within each KG classification from the UKESM1 temperatures. Note that climatological shifts lead to transitions between KG classes.

20

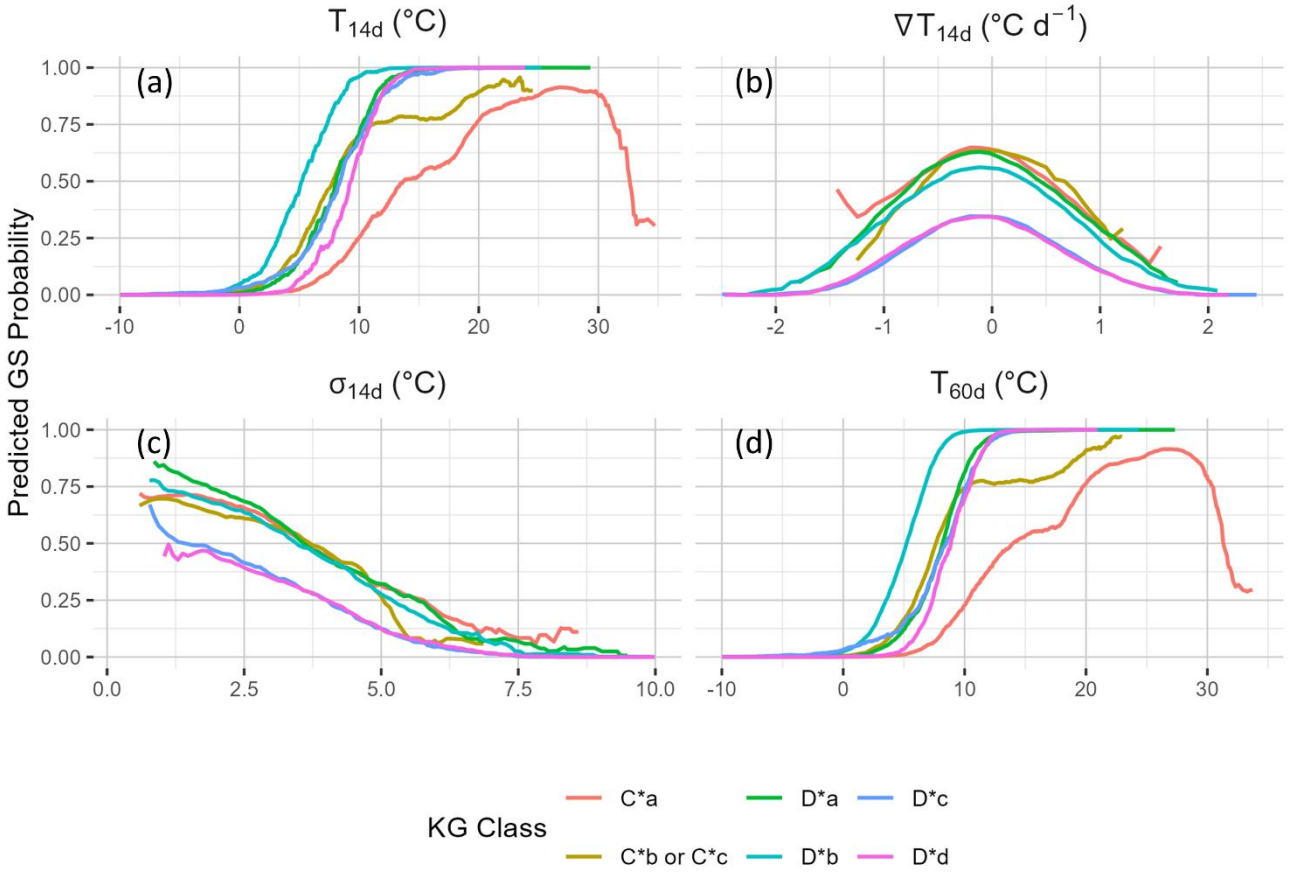

Figure S3. Probabilities of GS predicted from the binary classifier (model response) over each KG class. Profiles are obtained by first computing probabilities over 10,000 samples from the ERA5 dataset, then binning these probabilities, and finally smoothing the binned probabilities using a moving average.

25

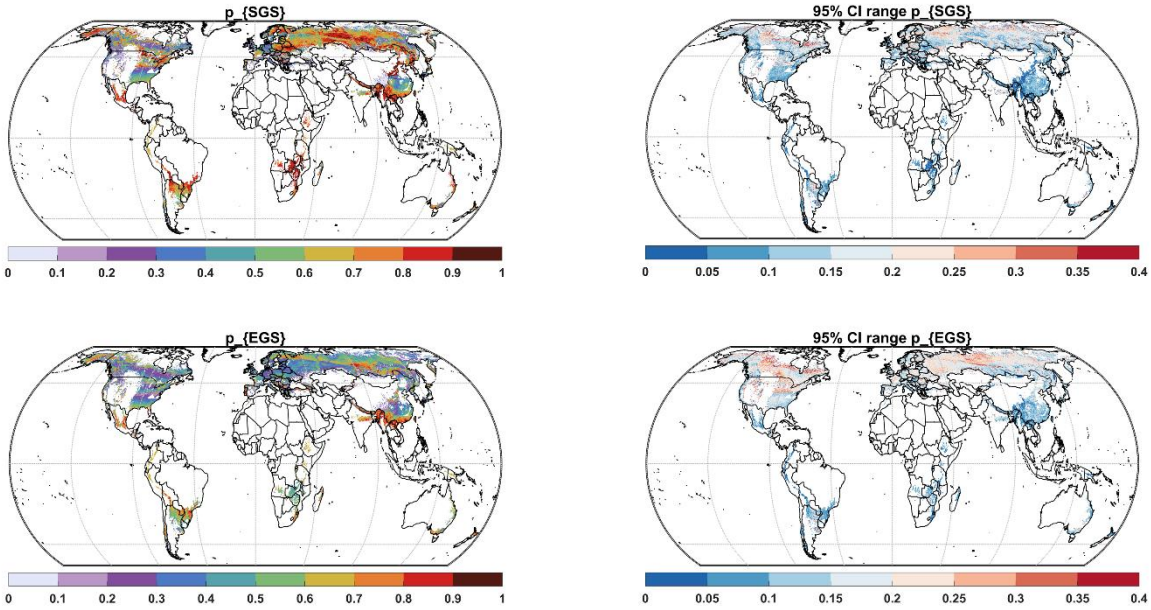

Figure S4. Node-level probability thresholds for GS transitions (p_{SGS}, p_{EGS}) and the corresponding 95% CI range.

Table S2. The parameter CI for GS-P and for GS-Lat, across the different KG classification.

	C*a	C*b ∨ C*c	D*a	D*b	D*c	D*d
GS-P						
μ_{SGS}	[0.548,0.561]	[0.522,0.551]	[0.587,0.627]	[0.572,0.598]	[0.567,0.599]	[0.56,0.648]
τ^2_{SGS}	[0.055,0.059]	[0.053,0.059]	[0.048,0.055]	[0.051,0.058]	[0.058,0.065]	[0.042,0.056]
σ^2_{SGS}	[0.011,0.013]	[0.014,0.017]	[0.027,0.034]	[0.027,0.033]	[0.028,0.034]	[0.03,0.044]
μ_{EGS}	[0.491,0.517]	[0.534,0.576]	[0.338,0.409]	[0.375,0.434]	[0.456,0.527]	[0.392,0.509]
τ^2_{EGS}	[0.038,0.044]	[0.035,0.045]	[0.031,0.039]	[0.028,0.035]	[0.038,0.047]	[0.019,0.041]
σ^2_{EGS}	[0.014,0.018]	[0.017,0.024]	[0.039,0.055]	[0.041,0.051]	[0.035,0.049]	[0.036,0.059]
GS-Lat		**NH**			**SH**	
$\beta_{0,SGS}$		[19.19,19.63]			[296.67,299.11]	
$\beta_{1,SGS}$		[1.92,1.93]			[-1.41,-1.34]	
$\beta_{2,SGS}$		[10,10.14]			[-8.97,-7.94]	
$\beta_{0,EGS}$		[341.81,342.46]			[196.24,198.29]	
$\beta_{1,EGS}$		[-1.14,-1.13]			[-1.31,-1.25]	
$\beta_{2,EGS}$		[-10.05,-9.84]			[-6.29,-5.42]	

Table S3. MB (Model – MODIS), MAE, and percentage of failed instances in predicting SGS and EGS over each KG class, calculated over the validation dataset. The metrics reported here are adjusted similarly to the loss function (Eq. A2) using the percentage of failed instances: MAE and MB are multiplied by the penalization factor, while ρ is divided.

	KG classification	**C*a**	**C*b ∨ C*c**	**D*a**	**D*b**	**D*c**	**D*d**	**Global**
	Validation dataset size	97,421	56,159	25,105	168,075	230,493	4,960	582,213
Metric	**Model**							
Failed pred (%)	GS-Lin2	2.01	31.78	0.00	0.22	0.45	0.00	3.64
	GS-BC2	0.00	0.13	0.00	0.00	1.22	0.00	0.49
	GS-P	0.54	2.49	0.00	0.03	0.09	0.00	0.37
	GS-Lat	0.00	0.00	0.00	0.00	0.00	0.00	0.00
MB (d)	GS-Lin2	23.5	78.7	8.7	12.8	2.0	0.5	12.9
	GS-BC2	1.4	-0.6	-0.4	2.5	-1.7	0.7	0.2
	GS-P	-15.4	-18.2	-1.4	-0.1	-1.3	-0.1	-4.8
	GS-Lat	11.0	44.6	3.2	12.1	-11.6	-5.2	5.1
MAE (d)	GS-Lin2	53.3	90.8	13.0	15.5	11.3	6.5	23.7
	GS-BC2	17.3	23.6	6.0	7.2	10.0	3.2	11.5
	GS-P	22.3	39.1	4.9	4.9	5.6	3.0	11.2
	GS-Lat	28.0	53.1	9.4	15.3	15.0	5.9	20.6
ρ	GS-Lin2	0.73	0.44	0.54	0.58	0.32	0.66	0.67
	GS-BC2	0.95	0.90	0.65	0.72	0.56	0.70	0.91
	GS-P	0.92	0.68	0.82	0.87	0.85	0.81	0.85
	GS-Lat	0.94	0.86	0.16	0.35	0.59	0.56	0.84
	KG classification	**C*a**	**C*b ∨ C*c**	**D*a**	**D*b**	**D*c**	**D*d**	**Global**
	Validation dataset size	97,204	56,081	25,105	168,072	230,479	4,960	581,901
Metric	**Model**							
Failed Pred (%)	GS-Lin2	1.98	31.73	0.00	0.22	0.45	0.00	3.63
	GS-BC2	16.95	0.13	0.00	0.00	0.00	0.00	2.84
	GS-P	0.52	2.47	0.00	0.03	0.09	0.00	0.37
	GS-Lat	0.00	0.00	0.00	0.00	0.00	0.00	0.00
MB (d)	GS-Lin2	-7.1	-6.5	-1.9	2.9	6.3	0.9	2.1
	GS-BC2	13.9	0.1	0.2	-1.2	0.6	-0.1	1.4
	GS-P	21.7	17.3	0.4	0.1	1.4	-0.3	5.8
	GS-Lat	20.2	7.1	-18.0	-17.4	15.5	18.7	4.6
MAE (d)	GS-Lin2	49.9	41.3	12.8	11.6	13.4	7.5	20.7
	GS-BC2	33.6	22.2	6.6	7.6	7.7	3.1	12.1
	GS-P	32.0	35.9	7.6	7.3	6.8	4.2	13.8
	GS-Lat	43.8	48.2	18.3	17.9	17.9	18.7	25.2
ρ	GS-Lin2	0.55	0.47	0.38	0.58	0.49	0.07	0.63
	GS-BC2	0.62	0.88	0.53	0.70	0.60	0.33	0.82
	GS-P	0.70	0.70	0.59	0.76	0.79	0.32	0.75
	GS-Lat	0.64	0.71	0.39	0.41	0.37	0.36	0.65

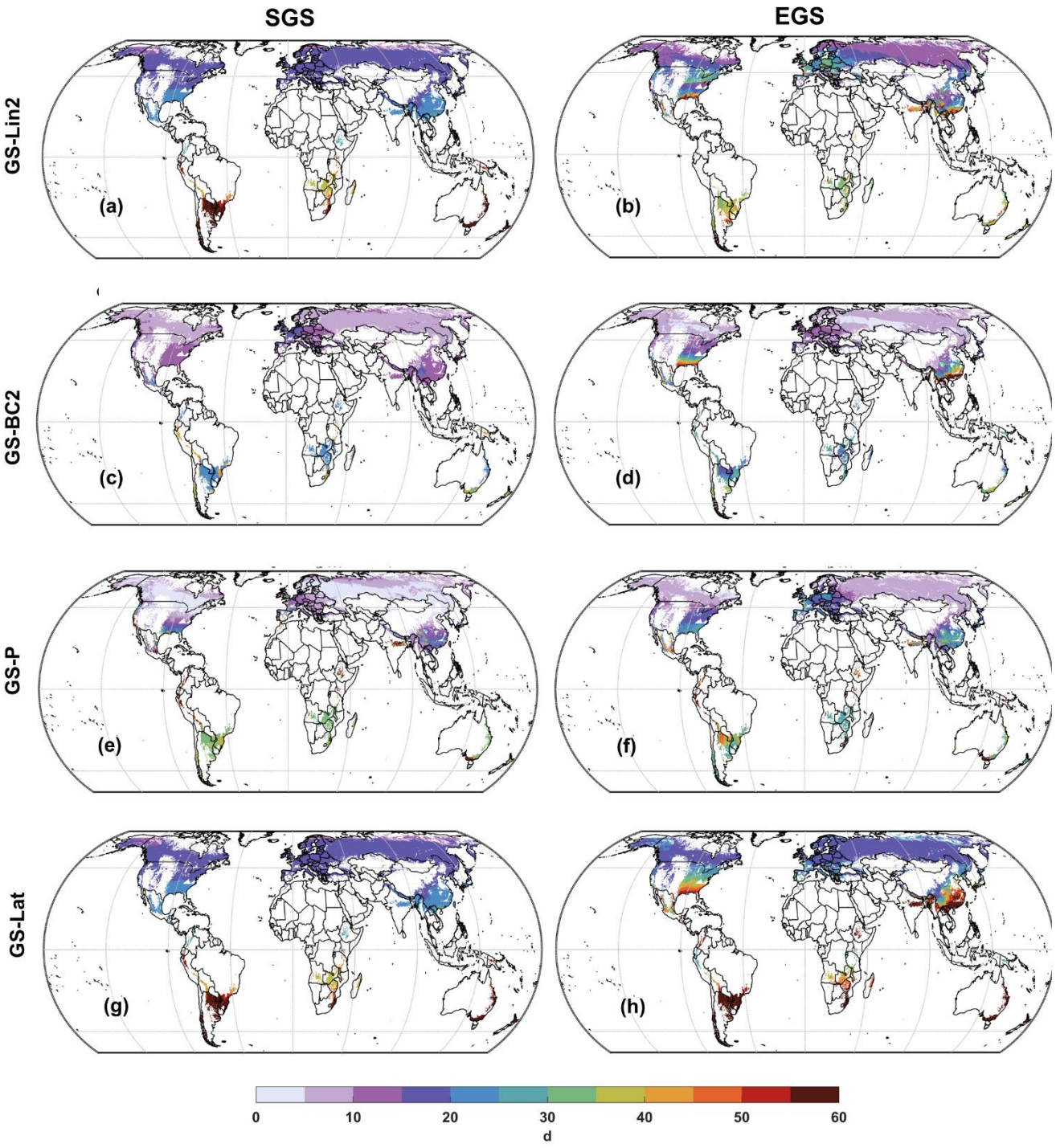

Figure S5. Estimated error spread (p_{95}) for SGS (first column) and EGS (second column), for the different GS models, using 2001-2023 ERA5 temperatures.

Table S4. Mean SGS, EGS and GS duration over each KG class during the preindustrial period (1850-1879), and relative shifts at 1985-2014 and 2071-2100 for the considered experiments. For the averaging, only nodes that did not transition to A climates and did not show any GS-flipping behaviour are considered. Here, the KG class identifies the nodes that were predominantly within that class during the preindustrial period.

Hemisphere	KG class	Preindustrial 1850-1879 historical	Differences with preindustrial period 1985-2014 historical	2071-2100 SSP1-2.6	2071-2100 SSP3-7.0	2071-2100 SSP5-8.5
			SGS			
NH	C*a	87.7	-2.0	-17.3	-33.2	-36.4
	C*b ∨ C*c	78.7	-3.1	2.4	-2.0	-8.3
	D*a	105.4	-0.9	-9.5	-20.4	-24.0
	D*b	115.5	-0.5	-5.2	-14.1	-17.5
	D*c	164.3	-0.9	-23.9	-35.7	-41.0
	D*d	182.0	-2.3	-20.3	-29.7	-37.9
SH	C*a	259.3	-6.7	-20.4	-33.8	-43.2
	C*b ∨ C*c	232.3	2.3	7.7	17.4	17.4
	D*a	–	–	–	–	–
	D*b	238.7	5.1	18.3	-8.8	-11.1
	D*c	251.6	-5.2	3.3	-11.9	-22.0
	D*d	–	–	–	–	–
			EGS			
NH	C*a	307.0	3.4	18.7	29.2	28.6
	C*b ∨ C*c	315.8	1.6	-3.3	4.0	8.0
	D*a	299.7	1.9	10.9	21.1	24.2
	D*b	292.4	0.9	7.8	17.3	20.3
	D*c	248.0	0.5	24.6	38.5	43.6
	D*d	225.1	1.5	22.9	38.5	47.5
SH	C*a	152.7	6.5	12.8	16.6	10.7
	C*b ∨ C*c	153.1	0.4	4.0	7.0	5.8
	D*a	–	–	–	–	–
	D*b	133.0	0.3	-4.3	24.1	21.6
	D*c	128.6	5.1	-3.7	8.5	12.9
	D*d	–	–	–	–	–
			GS Duration			
NH	C*a	219.3	5.4	36.1	62.4	65.1
	C*b ∨ C*c	237.2	4.8	-5.7	6.0	16.3
	D*a	194.3	2.8	20.4	41.5	48.2
	D*b	176.8	1.4	12.9	31.4	37.8
	D*c	83.7	1.4	48.5	74.2	84.7
	D*d	43.0	3.8	43.2	68.3	85.4
SH	C*a	258.3	13.2	33.2	50.4	53.9
	C*b ∨ C*c	285.7	-1.9	-3.8	-10.4	-11.7
	D*a	–	–	–	–	–
	D*b	259.3	-4.8	-22.6	32.9	32.8
	D*c	242.0	10.2	-7.0	20.4	34.8
	D*d	–	–	–	–	–

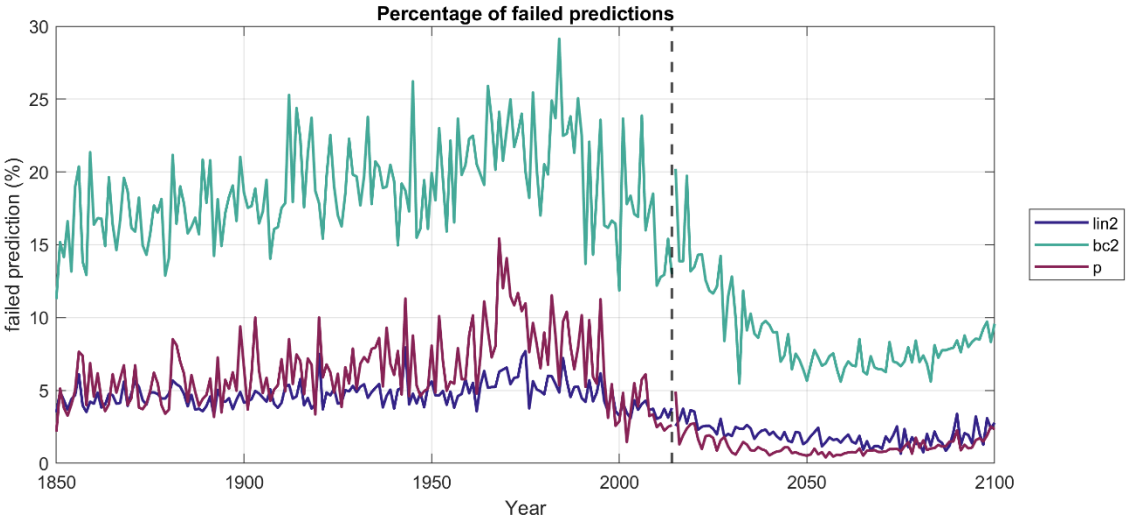

Figure S6. Percentage of failed predictions for the three temperature-based GS models (GS-Lin2, GS-BC2, GS-P) using UKESM1-0-LL temperatures from the historical (1850-2014) and SSP5-8.5 (2015-2100) experiment. Vertical dashed line indicates the separation year between the two experiments. The peak in failed prediction percentage around 1970 correspond to a small cooling of about 0.5°C in UKESM1-0-LL temperatures with respect to the previous years (data not shown).

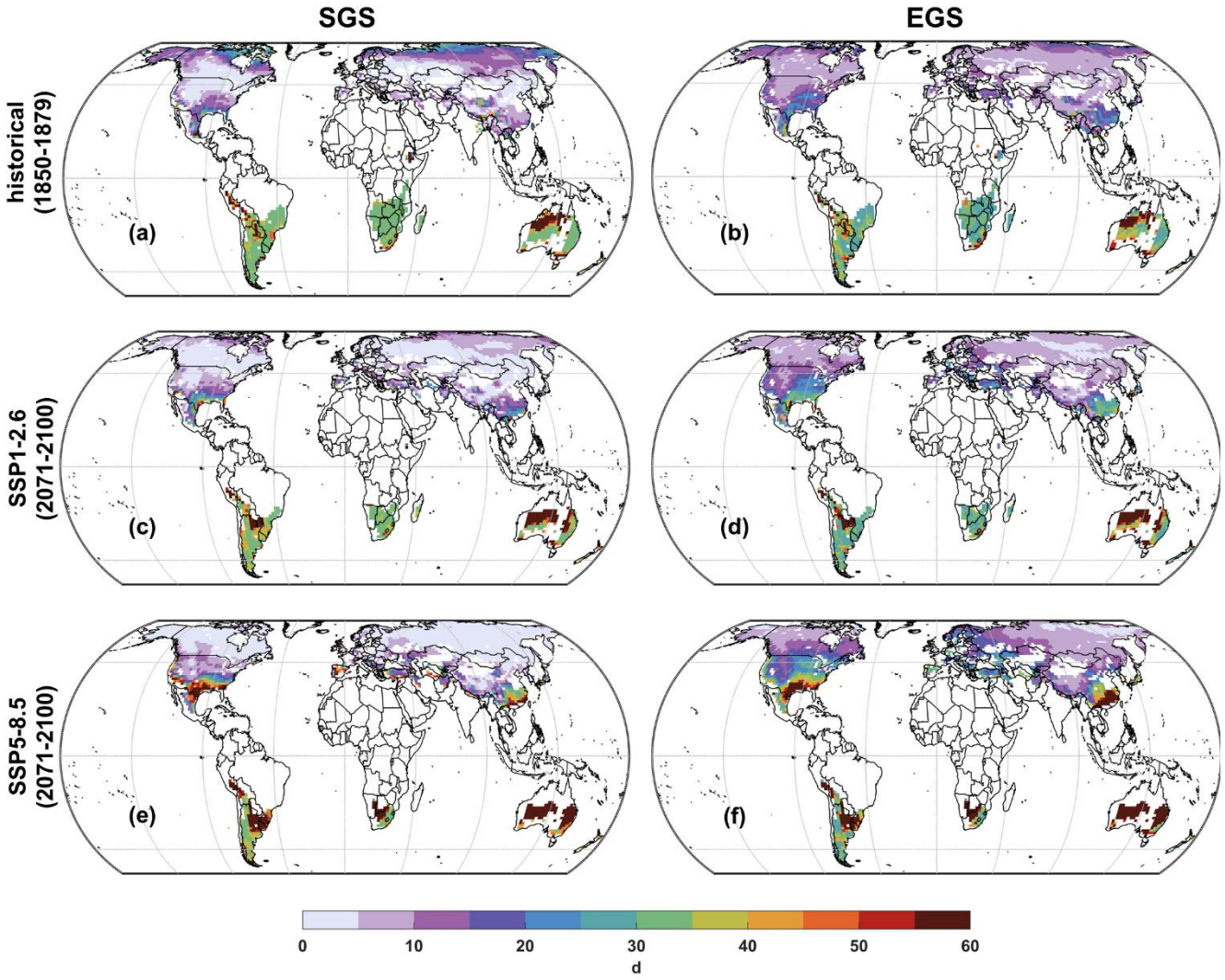

55

Figure S7. Estimated error spread (p_{95}) for SGS (first column) and EGS (second column), for GS-P over UKESM1-0-LL temperatures, for the preindustrial period (historical, 1850-1880; a,b), and for the end-century period (SSP1-2.6, c,d; SSP5-8.5, e,f).

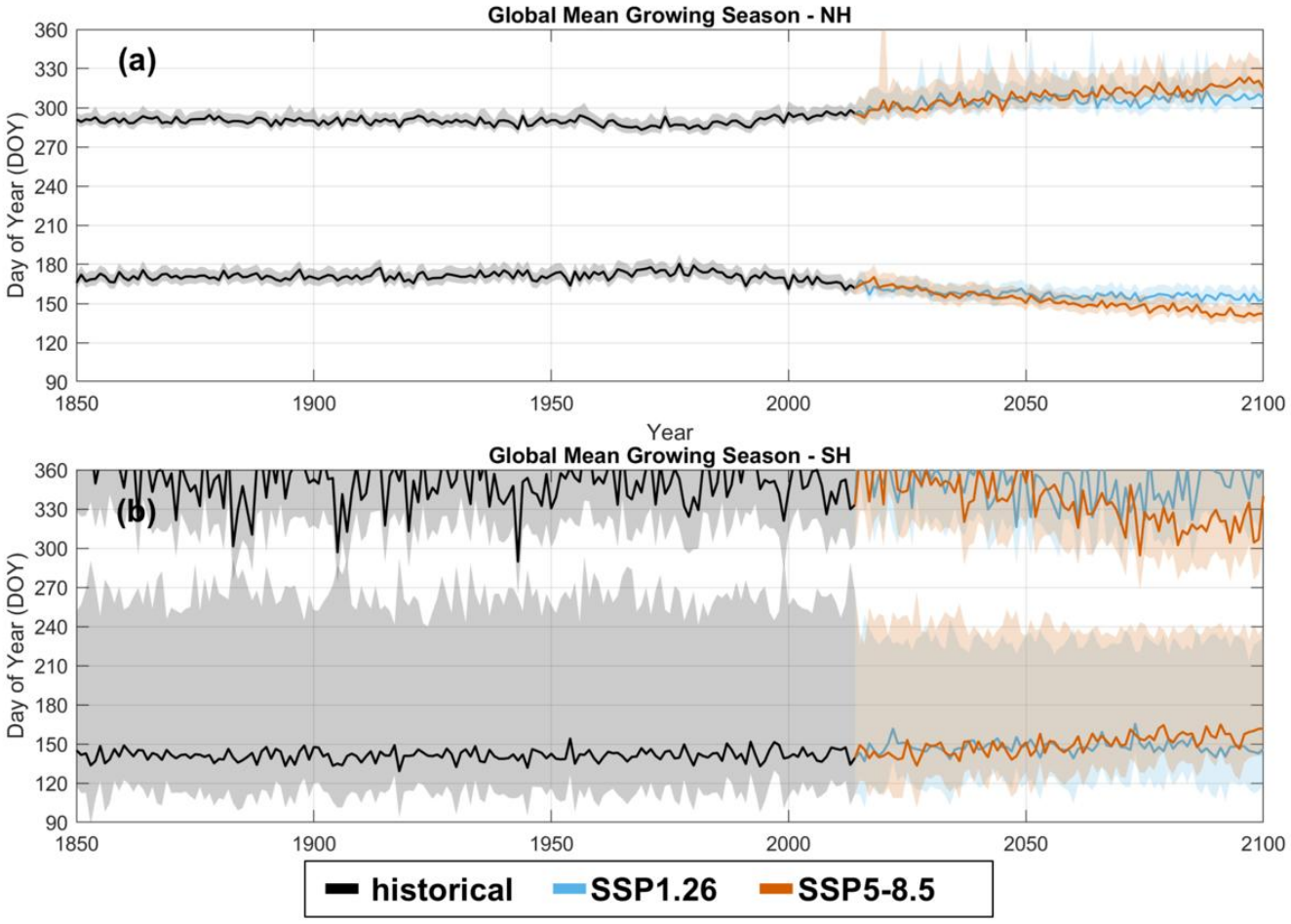

Figure S8. Area-weighed yearly averages of SGS and EGS from 1850 to 2100, for the Northern (a) and the Southern Hemisphere (c), as simulated by GS-Lin2 over UKESM1-0-LL temperatures, only considering non-KG transition, non-flipping nodes. In the NH, the bottom lines refer to the SGS, while the top lines refer to the EGS. In the SH, the order is reversed. Shaded areas indicate the 95% confidence interval.

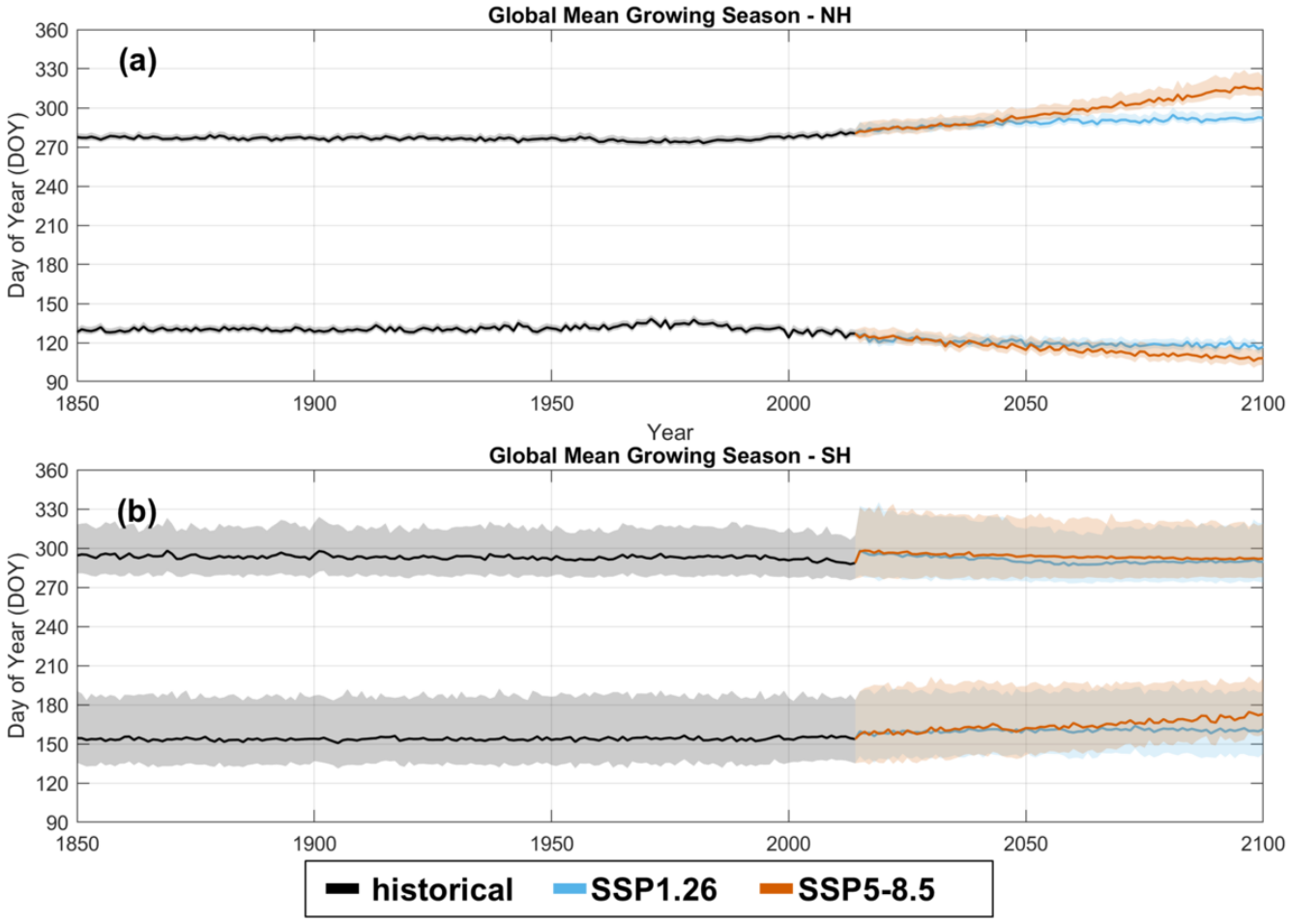

Figure S9. Area-weighed yearly averages of SGS and EGS from 1850 to 2100, for the Northern (a) and the Southern Hemisphere (c), as simulated by GS-BC2 over UKESM1-0-LL temperatures, only considering non-KG transition, non-flipping nodes. In the NH, the bottom lines refer to the SGS, while the top lines refer to the EGS. In the SH, the order is reversed. Shaded areas indicate the 95% confidence interval.